JACS
JOURNAL OF THE AMERICAN CHEMICAL SOCIETY
Communication
pubs.acs.org/JACS

Crystal Structure of a Human Prion Protein Fragment Reveals a Motif for Oligomer Formation

Marcin I. Apostol,*[,†,§] Kay Perry,[‡] and Witold K. Surewicz*[,†]

[†]Department of Physiology and Biophysics, Case Western Reserve University, Cleveland, Ohio 44106, United States
[‡]NE-CAT, Department of Chemistry and Chemical Biology, Cornell University, Argonne National Laboratory, Argonne, Illinois 60439, United States

Supporting Information

ABSTRACT: The structural transition of the prion protein from α-helical- to β-sheet-rich underlies its conversion into infectious and disease-associated isoforms. Here we describe the crystal structure of a fragment from human prion protein consisting of the disulfide-bond-linked portions of helices 2 and 3. Instead of forming a pair-of-sheets steric zipper structure characteristic of amyloid fibers, this fragment crystallized into a β-sheet-rich assembly of hexameric oligomers. This study reveals a never before observed structural motif for ordered protein aggregates and suggests a possible mechanism for self-propagation of misfolded conformations by such non-amyloid oligomers.

Amyloid fibers and nonamyloid oligomers have been shown to be associated with a number of "conformational diseases", including Alzheimer's, Parkinson's, and prion. Current evidence suggests that, at least in some cases, nonamyloid oligomers rather then amyloids may be the primary toxic species.[1] Prion diseases are particularly intriguing because aggregates of the prion protein (PrP) can be both toxic and infectious, with emerging evidence suggesting that these two traits are carried out by different types of aggregated species.[2] Furthermore, there are indications that small oligomers of PrP may be more infectious than larger fibrillar aggregates.[3]

Elucidating high-resolution structures of polypeptides in amyloid or oligomer conformations presents a formidable challenge for current structural biology techniques. Recently, an approach that reduces the complexity of aggregation-prone regions of proteins by dissecting them into smaller parts has illustrated that investigations into their atomic structures can be amenable to X-ray crystallography. While structural studies with relatively short segments would be of limited value for learning about the overall structure and function of globular proteins, structures of segments from the amyloidogenic regions of proteins have shed important new light on the molecular mechanisms of aggregation into amyloid fibers and oligomers. This approach has provided atomic insight into the assembly of amyloid fibers with numerous structures.[4−11] These have defined a common "steric zipper" motif characterized by a pair of β-sheets that extend indefinitely along the length of a fiber and a self-complementary interface between them composed of tightly interacting side chains.[4,5] Although the consensus properties of nonamyloid oligomers inferred from biophysical studies include a multimeric assembly typically described as β-sheet-rich,[12] until recently their structural organization has been elusive. The atomic-resolution structure of "cylindrin", formed from a segment of αB-crystallin, has provided an example of one possible oligomeric architecture.[13]

In the present study, we sought to gain structural insight into the role that the conserved intramolecular disulfide bond in PrP may play during the conversion of PrP into misfolded aggregates. In the normal form of the prion protein, PrP^{C}, the disulfide bond bridges two long α helices, α2 and α3 [Figure S1a in the Supporting Information (SI)]. However, during the formation of both amyloid fibrils[14,15] and oligomers from recombinant PrP in vitro,[16] these helices have been shown to undergo a vast structural rearrangement into a β-sheet structure. Recent evidence has suggested a similar conformational change in this region of the protein upon conversion to the infectious PrP^{Sc} isoform,[17] although alternative structural models have also been proposed.[18,19] Here we describe the 1.4 Å crystal structure (Table S1 in the SI) of DBPrP, a fragment from portions of α2 and α3 of human PrP corresponding to two discontinuous segments, ^{177}HDCVNI^{182} and ^{211}EQMCIT^{216}, that are covalently linked by a disulfide bond between Cys179 and Cys214 (Figure S1). Instead of forming a pair-of-sheets steric zipper reflective of amyloid fibers, the DBPrP fragment assembled into distinct β-sheet oligomers.

The crystal structure of DBPrP reveals a structural motif that was not observed in any previously crystallized amyloidogenic fragment. Six DBPrP fragments were found in the asymmetric unit of the crystal, each one making up a subunit of a hexameric oligomer. The overall structural organization of this hexamer is that of three four-stranded, antiparallel β-sheets arranged like the faces of a triangular prism (Figure 1a). The subunits form similar contacts between each other, and their assembly can be described as a trimer of dimers (D_3 point group symmetry) in which each four-stranded β-sheet is formed by association of two subunits along a twofold axis, and the hexamer results from association of dimeric β-sheets along a threefold axis (Figure 1).

The assembly of DBPrP fragments into prismatic hexamers is driven by maximization of hydrogen bonding and burial of hydrophobic side chains (Figure 1b). Figure 1c,d shows the consensus pattern of hydrogen bonding between strands in each of the antiparallel sheets, illustrating that their arrange-

Received: March 29, 2013
Published: June 28, 2013

   dx.doi.org/10.1021/ja403001q | J. Am. Chem. Soc. 2013, 135, 10202−10205

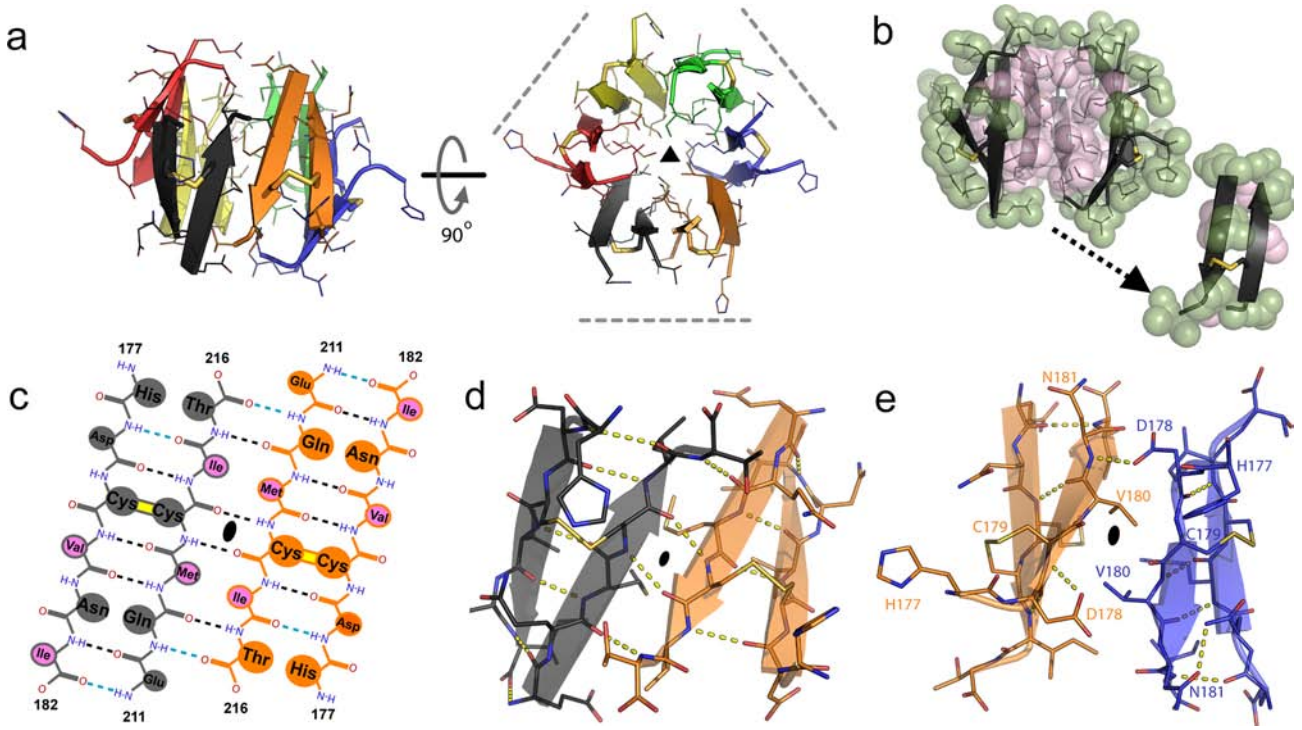

Figure 1. The structure of the hexameric oligomer formed by DBPrP fragments reveals a symmetric, tightly packed, prismatic assembly of β-sheets. (a) The hexamer is shown in two orientations: (left) side view of the prismatic assembly; (right) view down its quasisymmetric threefold axis (represented as a triangle). Dashed gray lines are intended to draw attention to the three four-stranded β-sheets that define the hexamer. The main chain and side chains are represented as cartoon β-strands and sticks, respectively. The subunits A−F are shown in different colors and arranged clockwise starting with chain A in orange. This color scheme is consistent with (c−e). (b) A side view of the oligomer with one segment removed reveals the tight complementary packing of hydrophobic side chains (pink spheres) in the interior and the exclusion of hydrophilic side chains (green spheres) to the exterior. (c) A schematic representation of one dimeric β-sheet illustrates the arrangement of hydrogen bonds between strands (dashed lines). Hydrogen bonds drawn in light blue are not observed in all six subunits within the hexamer because of the conformational flexibility of the strand termini. Side chains that protrude toward the exterior of the hexamer are depicted as larger circles. Smaller pink circles highlight hydrophobic residues that form a hydrophobic cluster along one of its interior faces. The black oval represents the twofold symmetry within the association of two subunits. (d) A molecular stick representation with a transparent overlay of cartoon β-strands shows the same dimeric β-sheet diagrammed in (c). (e) A similar molecular representation of the interaction between edge strands of two adjacent β-sheets shows that the Asp178 side chain twists away from the hydrophobic interior of the hexamer. In doing so, it forms a hydrogen bond to the peptide backbone, preventing the association of edge strands around the circumference of the hexamer.

ment allows for pairing of nearly all intra- and intermolecular backbone hydrogen-bond donors and acceptors except those present on the outer-edge strands. In this arrangement of strands, hydrophobic residues (Val180, Ile182, Met213, and Ile215) appear as a cluster on the interior face of the dimeric β-sheet (Figure 1c). The threefold assembly of these sheets along these clusters forms a dry interface, burying ~40% of the total surface area of each subunit. Furthermore, the shape complementarity (S_c) of the buried surfaces indicates tight interactions in the self-complementary association of the hydrophobic side chains comparable to those found at the dry interface of steric zippers (Table S2). Hydrophilic residues face the outside of the hexamer and interact extensively with solvent molecules (Figure S2). A closed topology of hydrogen bonding within the hexamer is prevented by residue Asp178, which faces the hydrophobic interior of the hexamer but twists away in order to avoid burying its charged headgroup. In doing so, it forms hydrogen bonding interactions to the peptide backbone of edge strands at the interface of the sheets and obstructs the formation of a continuous β-sheet around the hexamer (Figure 1e). As a result, the hexamer possesses open edge β-strands.

The hexameric structure of the DBPrP fragment was also found in solution. In size-exclusion chromatography experiments performed at physiological pH, the DBPrP fragment eluted as one distinct peak with a retention volume corresponding to a size larger than expected for a 1.4 kDa monomer (Figure S3a). The elution profile was independent of fragment concentration, indicating that this multimeric species was not in equilibrium with the monomer, at least over the concentration range tested (0.5−4 mg/mL). The peak had a elution volume similar to that of the aprotinin standard. Even though the molecular mass of aprotinin is ~6.5 kDa (i.e., smaller than that expected for the DBPrP hexamer), the radius of gyration of 11.2 Å calculated from its crystal structure (PDB entry 4PTI) is nearly equal to that calculated for the crystal structure of the DBPrP hexamer (10.8 Å). Thus, the similar elution volumes of aprotinin and DBPrP suggest that, as in the crystal, DBPrP exists as a hexamer in solution. This was further corroborated by native electrospray mass spectrometry experiments showing only a single stable oligomer with a mass of 8.5 kDa (Figure S3b,c), consistent with a hexamer. Together, these experiments indicate that in solution the DBPrP fragment forms a monodisperse population of hexamers with the same compact shape as observed in the crystal structure.

Although the hexameric assembly of DBPrP fragments is the effective unit of crystal growth, notable contact occurs between hexamers through their open edge strands. Within each DBPrP

dx.doi.org/10.1021/ja403001q | J. Am. Chem. Soc. 2013, 135, 10202−10205

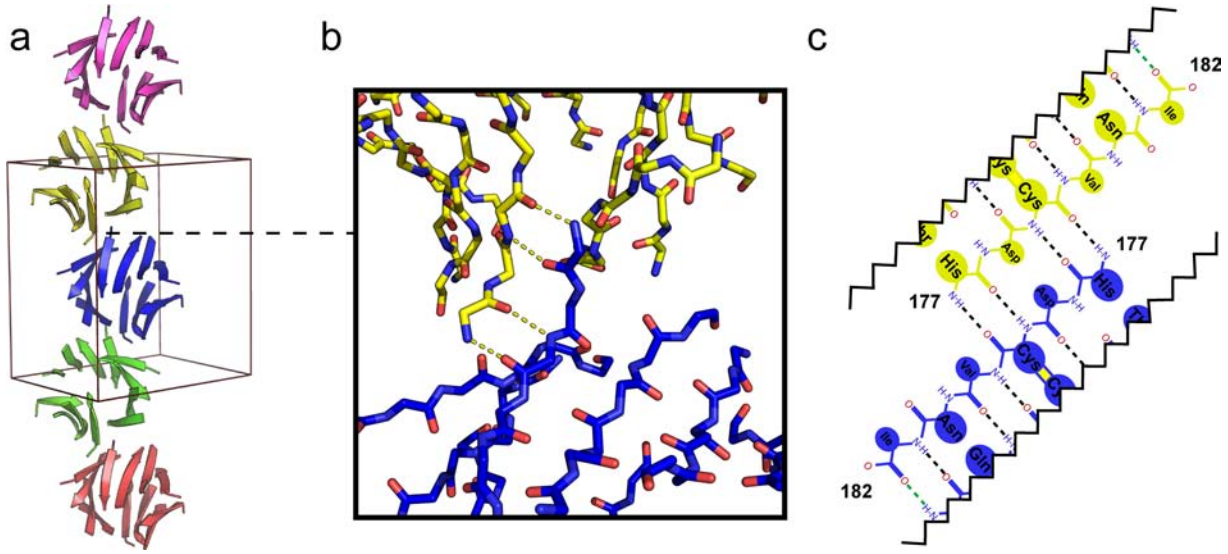

Figure 2. Interactions between hexamers are mediated through backbone hydrogen bonding. (a) A cartoon representation of symmetry-related hexamers (shown in different colors) illustrates their head-to-tail association along the *c* axis of the unit cell (gray box). (b) A detailed molecular view of one of these interactions shows that they are mediated through hydrogen bonding of the peptide backbone between two edge strands of adjacent hexamers, forming a short antiparallel β-sheet. (c) A schematic of this interaction shows the pattern of backbone hydrogen bonds between His177 and Cys179 from the two involved edge strands. The diagram is cut off where the interactions are the same as those described for individual hexamers (Figure 1).

fragment, as Asp178 twists away from the hydrophobic core of the hexamer, it perturbs the N-terminal portion the edge β-strands on which it is located, allowing the exposed edge strands to form hydrogen bonds with identical strands on adjacent hexamers (Figure 2a). This interaction creates a small antiparallel β-sheet stabilized by intermolecular backbone hydrogen bonds between residues His177 and Cys179 (Figure 2b,c). Although any of the six edge strands in the hexamer can form such interactions, only two strands do so, linking the hexamers together in a head-to-tail fashion. This head-to-tail assembly leads to a filament-like morphology throughout the crystal that, unlike in amyloid fibrils, does not have the alignment of β-strands perpendicular to the axis of elongation.

The DBPrP hexamer presented here represents a never-before-observed structural motif for nonamyloid oligomers. As previously postulated,[20] the organization of β-sheets into such oligomers may allow for many more degrees of freedom in terms of sheet-to-sheet packing arrangements compared to fibrillar (amyloid) aggregates, of which there are eight classes.[5] The recently described "cylindrin" structures of toxic oligomers formed by an 11-residue segment of αB crystallin reveal one such possible arrangement with characteristics of the β-barrel fold.[13] The DBPrP hexamer shows yet another possible type of structural organization for β-sheet oligomers that bears a striking similarity to the structural motif found in a handful of globular proteins, in which a prismlike association of three four-stranded β-sheets has been classified as a β-prism I fold.[21] The cylindrin and DBPrP hexamer structures represent two possible structural classes for β-sheet oligomers identified to date. These distinct structural arrangements may contribute to the great polymorphism described for these types of protein aggregates.[22]

Although structurally distinct, the oligomeric assemblies of cylindrins and DBPrP share some structural commonalities. Both are symmetric hexamers, the cylindrin with six strands and the DBPrP hexamer with 12 strands per oligomer. Furthermore, both have features in common with steric zippers, including a tight, self-complementary association of β-sheets at a dry interface. This suggests that aggregation through self-complementary interactions may be an innate property of polypeptides in both amyloid and nonamyloid oligomers. However, a major difference between these two structural motifs is that cylindrin has a closed β-sheet topology in which the first strand is hydrogen-bonded to the last one, whereas the DBPrP hexamer has exposed edge strands that promote the association of hexamers into larger assemblies, the implications of which are described below.

Globular proteins have evolved molecular features to prevent aggregation through the exposed edges of β-sheets.[23] In aberrant misfolded forms of proteins where evolution has not intervened, such as those represented by steric zippers and the DBPrP oligomer described herein, exposed β-sheet edges provide nucleation elements for further association. The assembly of DBPrP hexamers illustrates how the specific hydrogen-bonding interactions between exposed β-strand edges facilitates the formation of high-molecular-weight aggregates composed of identical oligomeric building blocks. This type of interaction could potentially explain the great heterogeneity of sizes and various morphologies reported for nonamyloid oligomers,[22] including that of infectious PrP^{Sc}.[3] Interestingly, studies of a partially disaggregated form of infectious PrP^{Sc} revealed oligomers with threefold symmetry[18] similar to that found in the DBPrP hexamer.

The crystal structure of the DBPrP hexamer shows one possible conformation of this fragment of PrP in a β-sheet-rich conformation and provides insight into how it can scaffold the assembly of the protein into a similar structure. To illustrate the latter point, we created a model showing how the entire C-terminal amyloidogenic region of PrP[14,24] can be accommodated into a threefold-symmetric hexameric oligomer scaffolded on the DBPrP fragment structure (Figure S4). Since there is evidence that oligomers share common structural features,[25] it can be imagined that other amyloidogenic proteins where

dx.doi.org/10.1021/ja403001q | J. Am. Chem. Soc. 2013, 135, 10202−10205

oligomer formation has been observed may also adopt similar conformations.

The structural organization of the DBPrP fragment described here allows us to speculate on a general mechanism by which misfolded protein conformations could self-propagate within the context of nonamyloid oligomers. This issue is of particular importance to the understanding of prion disease. The infectious PrP^{Sc} isoform in prion disease replicates by binding to the cellular PrP^{C} isoform and templating its conversion to the PrP^{Sc} structure in a process that is often modeled by an analogy to seeded polymerization of amyloid fibrils.[26,27] This templating takes place at the open β-strands at the ends of amyloid fibers, forming very stable non-native interactions between misfolded proteins. However, models based on this analogy are complicated by the uncertainty regarding the molecular nature of infectious prion particles: while some strains of mammalian prions have characteristics of amyloid fibers, in others these characteristics were not detected.[28] Furthermore, it has been shown that highest infectivity per mass unit is associated with prion particles that are substantially smaller than long fibrils.[3] These observations, together with the very limited infectivity of amyloid fibers formed from recombinant PrP in vitro,[29] implicate nonamyloid oligomers in the process of infectivity and underscore the need for alternative (i.e., nonamyloid-based) models for the self-propagation of mammalian prions. The DBPrP structure presented here shows how oligomers, just like amyloid fibers, can possess open β-strands that can template the growth of larger assemblies of misfolded protein. Hence, this novel structural motif for nonamyloid aggregation provides a paradigm for an alternative basis for the self-propagation of misfolded proteins through such nonamyloid aggregates.

■ ASSOCIATED CONTENT

Supporting Information

Details of crystallization, data collection, gel filtration, and mass spectrometry; additional figures; and tables of crystallographic data collection and refinement statistics as well as structural characteristics. This material is available free of charge via the Internet at http://pubs.acs.org. Structures have been deposited in the Protein Data Bank as entries 4E1H and 4E1I.

■ AUTHOR INFORMATION

Corresponding Author

marcinapostol@yahoo.com; witold.surewicz@case.edu

Present Address

[§]M.I.A.: Department of Molecular Cardiology, Lerner Research Institute, Cleveland Clinic, 9500 Euclid Avenue, Cleveland, OH 44195, USA.

Notes

The authors declare no competing financial interest.

■ ACKNOWLEDGMENTS

This work was supported by U.S. National Institutes of Health Grants NS044158 and NS074317 to W.K.S. Research conducted at the Advanced Photon Source on NE-CAT beamlines was supported by NIH Grants 5P41 RR015301-10 and 8P41 GM103403-10 and U.S. Department of Energy Contract DE-AC02-06CH11357.

■ REFERENCES

(1) Haass, C.; Selkoe, D. J. *Nat. Rev. Mol. Cell Biol.* **2007**, *8*, 101.
(2) Sandberg, M. K.; Al-Doujaily, H.; Sharps, B.; Clarke, A. R.; Collinge, J. *Nature* **2011**, *470*, 540.
(3) Silveira, J. R.; Raymond, G. J.; Hughson, A. G.; Race, R. E.; Sim, V. L.; Hayes, S. F.; Caughey, B. *Nature* **2005**, *437*, 257.
(4) Nelson, R.; Sawaya, M. R.; Balbirnie, M.; Madsen, A. Ø.; Riekel, C.; Grothe, R.; Eisenberg, D. *Nature* **2005**, *435*, 773.
(5) Sawaya, M. R.; Sambashivan, S.; Nelson, R.; Ivanova, M. I.; Sievers, S. A.; Apostol, M. I.; Thompson, M. J.; Balbirnie, M.; Wiltzius, J. J. W.; McFarlane, H. T.; Madsen, A. Ø.; Riekel, C.; Eisenberg, D. *Nature* **2007**, *447*, 453.
(6) Wiltzius, J. J. W.; Sievers, S. A.; Sawaya, M. R.; Cascio, D.; Popov, D.; Riekel, C.; Eisenberg, D. *Protein Sci.* **2008**, *17*, 1467.
(7) Wiltzius, J. J. W.; Landau, M.; Nelson, R.; Sawaya, M. R.; Apostol, M. I.; Goldschmidt, L.; Soriaga, A. B.; Cascio, D.; Rajashankar, K.; Eisenberg, D. *Nat. Struct. Mol. Biol.* **2009**, *16*, 973.
(8) Ivanova, M. I.; Sievers, S. A.; Sawaya, M. R.; Wall, J. S.; Eisenberg, D. *Proc. Natl. Acad. Sci. U.S.A.* **2009**, *106*, 18990.
(9) Apostol, M. I.; Wiltzius, J. J. W.; Sawaya, M. R.; Cascio, D.; Eisenberg, D. *Biochemistry* **2011**, *50*, 2456.
(10) Colletier, J.-P.; Laganowsky, A.; Landau, M.; Zhao, M.; Soriaga, A. B.; Goldschmidt, L.; Flot, D.; Cascio, D.; Sawaya, M. R.; Eisenberg, D. *Proc. Natl. Acad. Sci. U.S.A.* **2011**, *108*, 16938.
(11) Apostol, M. I.; Sawaya, M. R.; Cascio, D.; Eisenberg, D. *J. Biol. Chem.* **2010**, *285*, 29671.
(12) Fändrich, M. *J. Mol. Biol.* **2012**, *421*, 427.
(13) Laganowsky, A.; Liu, C.; Sawaya, M. R.; Whitelegge, J. P.; Park, J.; Zhao, M.; Pensalfini, A.; Soriaga, A. B.; Landau, M.; Teng, P. K.; Cascio, D.; Glabe, C.; Eisenberg, D. *Science* **2012**, *335*, 1228.
(14) Cobb, N. J.; Sönnichsen, F. D.; McHaourab, H.; Surewicz, W. K. *Proc. Natl. Acad. Sci. U.S.A.* **2007**, *104*, 18946.
(15) Tycko, R.; Savtchenko, R.; Ostapchenko, V. G.; Makarava, N.; Baskakov, I. V. *Biochemistry* **2010**, *49*, 9488.
(16) Chakroun, N.; Prigent, S.; Dreiss, C. A.; Noinville, S.; Chapuis, C.; Fraternali, F.; Rezaei, H. *FASEB J.* **2010**, *24*, 3222.
(17) Smirnovas, V.; Baron, G. S.; Offerdahl, D. K.; Raymond, G. J.; Caughey, B.; Surewicz, W. K. *Nat. Struct. Mol. Biol* **2011**, *18*, 504.
(18) Govaerts, C.; Wille, H.; Prusiner, S. B.; Cohen, F. E. *Proc. Natl. Acad. Sci. U.S.A.* **2004**, *101*, 8342.
(19) DeMarco, M. L.; Daggett, V. *Proc. Natl. Acad. Sci. U.S.A.* **2004**, *101*, 2293.
(20) Liu, C.; Sawaya, M. R.; Cheng, P.-N.; Zheng, J.; Nowick, J. S.; Eisenberg, D. *J. Am. Chem. Soc.* **2011**, *133*, 6736.
(21) Shimizu, T.; Morikawa, K. *Trends Biochem. Sci.* **1996**, *21*, 3.
(22) Fändrich, M. *J. Mol. Biol.* **2012**, *421*, 427.
(23) Richardson, J. S.; Richardson, D. C. *Proc. Natl. Acad. Sci. U.S.A.* **2002**, *99*, 2754.
(24) Lu, X.; Wintrode, P. L.; Surewicz, W. K. *Proc. Natl. Acad. Sci. U.S.A.* **2007**, *104*, 1510.
(25) Kayed, R.; Head, E.; Thompson, J. L.; McIntire, T. M.; Milton, S. C.; Cotman, C. W.; Glabe, C. G. *Science* **2003**, *300*, 486.
(26) Jarrett, J. T.; Lansbury, P. T. *Cell* **1993**, *73*, 1055.
(27) Hall, D.; Edskes, H. *J. Mol. Biol.* **2004**, *336*, 775.
(28) Bett, C.; Joshi-Barr, S.; Lucero, M.; Trejo, M.; Liberski, P.; Kelly, J. W.; Masliah, E.; Sigurdson, C. J. *PLoS Pathog.* **2012**, *8*, No. e1002522.
(29) Legname, G.; Baskakov, I. V.; Nguyen, H.-O. B.; Riesner, D.; Cohen, F. E.; DeArmond, S. J.; Prusiner, S. B. *Science* **2004**, *305*, 673.